ISSN (Online) 2456-1290
International Journal of Engineering Research in Mechanical and Civil Engineering (IJERMCE)
Special Issue
National Conference on Advances in Civil and Mechanical Engineering (NCACME 17)

A Review Paper on - Augmentation of Heat Transfer in Microchannel & Minichannel Heat Exchanger

[1] Akash A.Lokhande [2] S.M.Shaikh [3]R.H.Yadav
[1] PG Student,M.E.Heat Power, [2][3] Professor
[1][2][3] Dr.J.J.Magdum College of Engineering,Jaysingpur,Shivaji University,Kolhapur

Abstract:- **Microchannel Heat transfer has the very potential of wide applications in cooling high power density microchips in the CPU system, the micro power systems and even many other large scale thermal systems requiring effective cooling capacity. This is a result of the micro size of the cooling system which not only significantly reduces the weight load, but also enhances the capability to remove much greater amount of heat than any of large scale cooling systems. It has been recognized that for flow in a large scale channel, the heat transfer Nusselt number, which is defined as (hD/k), is a constant in the thermally developed region where h is the convective heat transfer coefficient, k is thermal conductivity of the fluid and D is the diameter of the channel. One can expect that as the size of the channel decrease, the value of convective heat transfer coefficient, h, becomes increasing in order to maintain a constant value of the Nusselt number. As the size of the channel reduces to micron or nano size, the heat transfer coefficient can increase thousand or million times the original value. This can drastically increase the heat transfer and has generated much of the interest to study microchannel heat transfer both experimentally and theoretically.**

I. INTRODUCTION

Heat Exchangers are the devices that facilitate the exchange of heat between two fluids that are at different temperatures while keeping them from mixing with each other. Heat Exchangers are commonly used in practice in a wide range of application, from heating & Air Conditioning systems in a household, to chemical processing & power production in large plants.

Types of Heat Exchangers:-

Heat Exchangers may be classified into several categories. One classification is according to fluid flow arrangement or relative direction of hot & cold fluid;

1.Parallel Flow
2.Counter Flow
3.Single Pass
4.Cross Flow.

The two major categories of heat exchangers are shell-and-tube exchangers and compact exchangers. Shell-and-tube exchangers are custom designed for virtually any capacity and operating condition, from high vacuums to ultrahigh pressures, from cryogenics to high temperatures, and for any temperature and pressure differences between the fluids, limited only by the materials of construction. They can be designed for special operating conditions: vibration, heavy fouling, highly viscous fluids, erosion, corrosion, toxicity, radioactivity, multi-component mixtures, etc. They are made from a variety of metal and non-metal materials, and in surface areas from less than 0.1 to 100,000 m^2 (1 to over 1,000,000ft^2). They have generally an order of magnitude less surface area per unit volume than the compact exchangers, and require considerable space, weight, support structure, and footprint.

Compact heat exchangers have a large heat transfer surface area per unit volume of the exchanger, resulting in reduced space, weight, support structure and footprint, energy requirement and cost, as well as improved process design, plant layout and processing conditions, together with low fluid inventory compared with shell-and-tube exchangers. From the operating condition and maintenance point of view, compact heat exchangers of different constructions are used for specific applications, such as for high temperature applications (up to about 850°C or 1550°F), high pressure applications (over 200 bars), and moderate fouling applications. A heat exchanger is a device to provide for transfer of internal thermal energy (enthalpy) between two or more fluids, between a solid surface and a fluid, or between solid particulates and a fluid, in thermal contact without external heat and work interactions. The fluids may be single compounds or mixtures. Typical applications involve heating or cooling of a fluid stream of concern, evaporation or condensation of single or multi-component fluid stream, and heat recovery or heat rejection from a system. In other applications, the objective may be to

ISSN (Online) 2456-1290
International Journal of Engineering Research in Mechanical and Civil Engineering (IJERMCE)
Special Issue
National Conference on Advances in Civil and Mechanical Engineering (NCACME 17)

sterilize, pasteurize, fractionate, distill, concentrate, crystallize, or control process fluid. In some heat exchangers, the fluids transferring heat are in direct contact. In other heat exchangers, heat transfer between fluids takes place through a separating wall or into and out of a wall in a transient manner. In most heat exchangers, the fluids are separated by a heat transfer surface and do not mix. Such exchangers are referred to as direct transfer type, or simply recuperators. Exchangers in which there is an intermittent flow of heat from the hot to cold fluid (via heat storage and heat rejection through the exchanger surface or matrix) are referred to as indirect transfer type or simply regenerators. The heat transfer surface is a surface of the exchanger core which is in direct contact with fluids and through which heat is transferred by conduction in a recuperator. The portion of the surface which also separates the fluids is referred to as a primary or direct surface. To increase heat transfer area, appendages known as fins may be intimately connected to the primary surface to provide an extended, secondary, or indirect surface. Thus, the addition of fins reduces the thermal resistance on that side and thereby increases the net heat transfer from the surface for the same temperature difference.

Multi port Mini-channel and Micro-channel Tubes are becoming more popular components in Heat exchangers. These Heat Exchangers are used in various industrial applications and are produced in large quantities with many different geometries and lengths and therefore they are relatively expensive. The ability to produce the tubes with external or internal fins with smaller wall thickness allows higher heat transfer area per unit volume of tube. Therefore Mini and Micro channels tubes ideal for use in compact light weight heat exchangers. The use of Mini or Micro-channels Heat Exchangers in Refrigeration equipment, offers the possibility of low refrigerant charge as well as high heat transfer and compact designs.

The distinction between Mini-channel and Micro-channel is given by Khandilkar, defines tubes with channel diameters between 0.001-0.2mm (200 μm To 10 μm) as Micro-channels, channel diameters between 0.2 -3mm (3 mm To 200 μm) as Minichannels. However, others prefer a diameter of 1mm as demarcation between Micro-channels and Minichannels.

Classification scheme of channels:-
Conventional channels Dh > 3mm
Minichannels 3 mm > Dh > 200 μm
Microchannels 200 μm > Dh > 10 μm
Transitional Microchannels 10 μm > Dh > 1 μm
Transitional Nanochannels 1 μm > Dh > 0.1 μm
Molecular Nanochannels 0.1 μm > Dh

They noted that Reynolds numbers at the channels were about two to three times higher than inlet in Laminar flow. The reason for this difference was given as rapid change of fluid properties along the channel length. According to their report, fully developed turbulence flow starts in the Reynolds number 1000-1500 and laminar to turbulent flow transition occur in the Reynolds number rang of 300- 800.

II. ENHANCEMENT TECHNIQUES FOR MICROCHANNELS AND MINICHANNELS

A] Passive Techniques

The passive enhancement techniques used in single-phase flow augmentation will be discussed in this section. Some of the basic techniques used for the passive enhancement include flow disruption, secondary flows, surface treatments, and entrance effects. Several of these techniques can be easily implemented into a microchannel or a minichannel.

1. Surface Roughness

One passive technique is to alter the characteristics of the heated surface. This method reduces the thermal boundary layer thickness and also aids in early transition into turbulent flow. The conventional way to alter the surface is to increase the roughness of the surface. The effective roughness ε/D ratio is increased to create a boundary layer influence. The roughness ratio can be very large in a microchannel. Therefore, the roughness structure could approach the channel diameter and cause adverse flow behaviour. This issue is a very active area of current research. Kandlikar et.al. (2003) studied the effect of surface roughness in a minichannel flow. They determined that the ε/D ratio has a bigger effect in smaller diameter channel than the same ε/D ratio in a conventional channel. Further information on the microfluidic physics is required for implementation. Champagne and Bergles (2001) presented an interesting work to develop a variable roughness enhancement structure. The idea utilized an insert constructed from a shape memory alloy (SMA), specifically Nickel Titanium. As the change in temperature increased, the insert would expand and increase the heat transfer enhancement. This concept could be expanded to minichannels and microchannels. Some SMAs could be inserted into the channels to provide a similar function.

2. Flow Disruptions

The inclusion of flow interruptions is perhaps the most attractive technique to incorporate. The flow disruptions provide increased mixing and also can serve to

ISSN (Online) 2456-1290
International Journal of Engineering Research in Mechanical and Civil Engineering (IJERMCE)
Special Issue
National Conference on Advances in Civil and Mechanical Engineering (NCACME 17)

trip the boundary layer causing flow transition. In conventional sized passages, the flow interruption can be achieved using flow inserts, flow disruptions along the sidewalls, and offset strip fins. These techniques are strong candidates for implementation in minichannels. The ability to manufacture smaller diameter wire has progressed enough to manufacture a thin wire, such as those for surgical applications, and insert a tightly coiled wire into a minichannel. The use of flow inserts in a microchannel maybe impractical due to the space requirements. The microchannel dimensions prove to be the limiting factor for the wire diameter currently available. Although, the basic concept in the flow inserts can be applied to microchannels. The flow disruption technique could find easy integration into microchannels using carefully constructed geometries. The feature size and geometry of objects improve as the achievable critical dimension is decreased. The sidewalls of the microchannel could contain flow obstacles that disrupt the boundary layer.

Another possibility is using flow obstacles in the bulk area of the microchannel. Obstructions with simple rectangular geometries and with circular geometries. The heights of these structures could vary to increase the secondary flows in the flow field. As the achievable critical dimensions in lithography are reduced, a more refined circular profile can be achieved. These geometries can be optimized and intermixed to achieve the maximum amount of heat transfer enhancement with the lowest pressure drop penalty.

3. Channel Curvature

Several researchers have demonstrated that heat transfer enhancement can be achieved by having a curved flow path. The traditional parabolic velocity profile is skewed due to the additional acceleration forces. This causes the angle between the gradients to decrease and facilitate enhancement. Sturgis and Mudawar (1999) demonstrated the enhancement in a curved channel. The radius of curvature was 32.3 mm and the channel had a cross section of 5.0 x 2.5 mm. The resulting hydraulic diameter is 3.33 mm. The enhancement reached as much as 26% for the curved channel versus a straight channel. This technique is not really practical in a large sized conventional passage. The application is a possibility in a minichannel for using return bend and such for compact heat exchangers. However, the greatest potential lies in a microchannel. The radius of curvature can be on the order of a few millimeters to centimeters but considered to be large compared to the channel diameter. The compact nature of the microchannel flow network could allow for a serpentine flow channels to utilize the curvature enhancement. This concept can be seen in the work involved in fabricating a microsystem gas chromatography column.

4. Re-entrant Obstructions

The entrance region of channels can also provide heat transfer enhancement. There are a few researchers that have reported the enhancement gained in the entrance region of a microchannel, Gui and Scaringe (1995). This technique could also find application in minichannels. However, the short lengths and low Reynolds numbers found in microchannel flows seem to be more appropriate. Gui and Scaringe (1995) reported heat transfer enhancement in microchannel heat sinks. The hydraulic diameters range from 221 μm to 388 μm. They suggested that the high heat transfer coefficients resulted from the decreased size, entrance effects, pre-existing turbulence at the inlet, and wall roughness. The short lengths in a microchannel could allow a design to build in entrance spaces in the flow network. The sudden expansion and contractions would generate entrance effects. This would cause the flow to be in a perpetual state of development and allow for heat transfer enhancement. The cavities could also be used for pressure measurements and possible mixing sites.

5. Secondary Flows

Many researchers have demonstrated that secondary flows within the flow field provide enhancement. This can be seen in conventional channels. This technique can be applied in minichannels using offset strip fins and chevron plates and further refinement for minichannels is possible. The optimal shape and pitch of such devices can continue to improve the heat transfer enhancement. The generation of secondary flows or swirl flows also has potential in microchannels. The geometry of the microchannel can be manipulated to produce secondary flow. Smaller channels are added between the main flow channels. Secondary flow will move from one channel to another via these channels. A second method for generating secondary flow comes from a conventional device. A venturi can be manipulated to generate secondary flow without external power and a major increase in pressure drop. The throat area is connected to the larger area section of an adjacent microchannel. The reduction in pressure at the throat area seen from the reduction in area will draw flow in from the larger area of the adjacent channel. This technique could also be utilized to increase fluid mixing or the addition of another flow stream to the main flow stream without the need for secondary flow pumping power. Once again, the pressure drop penalties could be a limiting factor for these devices.

ISSN (Online) 2456-1290
International Journal of Engineering Research in Mechanical and Civil Engineering (IJERMCE)
Special Issue
National Conference on Advances in Civil and Mechanical Engineering (NCACME 17)

6. Out of Plane Mixing

A technique being developed to increase binary fluid mixing could also be applied to the heat transfer enhancement in microchannels. Bondar and Battaglia (2003) have studied the effect of out of plane or three-dimensional mixing of two-phase flows in microchannels. They have achieved a high degree of fluid mixing. An example of a three-dimensional twisted microchannel is shown in Fig. 1. This work could provide a path to follow for single-phase heat transfer. The rotation of the fluid will promote mixing and therefore change the hydrodynamic and thermal gradients.

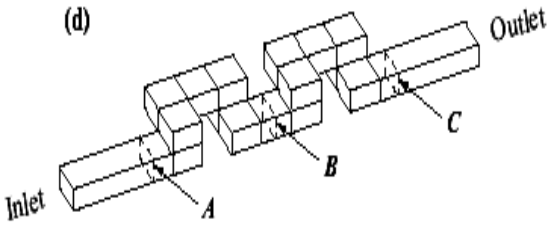

Fig. 1: Three-Dimensional Twisted Microchannel, Bondar and Battaglia (2003).

7. Fluid Additives

The addition of small particles to the fluid can sometimes provide heat transfer enhancement. The use of small particles containing a phase change material (PCM) to achieve heat transfer enhancement has been studied. The particles begin in the solid state. As the fluid temperature increases, the particles reach their melting point and begin to melt. The latent heat of fusion involved with the melting of the PCM creates an enhancement. In other words, the effective heat capacity of the fluid has changed due to the presence of the PCM.

Hu and Zhang (2002) studied the effect of microcapsules containing a PCM. The radius of the particles used was 50 μm in a 1.57 mm radius duct. Figure 8 shows the effect of particle concentration on the heat transfer enhancement. The figure shows the degree of heat transfer enhancement verses the non-dimensionalized axial coordinate, using the duct radius. This method works well in conventional channels. Smaller particles are being developed for use in minichannels and may possibly extended to microchannels.

B] Active Techniques

The active enhancement techniques used in single-phase flow augmentation will be discussed in this section. Generally, these techniques require additional, external input into the system. The input to the system could be in the form of power, electricity, RF signals, or external pumps.

1. Vibration

Vibration in the fluid or surface is another active technique that has been applied to conventional channel. The tubes in some conventional heat exchangers can vibrate and provide heat transfer enhancement. This technique could easily be applied to a minichannel heat exchanger. The smaller more compact nature of the tube bundles would allow for easier access for tube vibration The use of conventional external vibration generators in a microchannel is impractical due to the large sizes. However, a vibrating source could be integrated in a microchannel wall. The same technology that generates piezoelectric actuators could find application here. If a piezoelectric material can be embedded, deposited, or placed to act on the microchannel walls, the piezoelectric can be made to oscillate at different frequencies. This would generate surface vibrations and cause enhancement.

2. Electrostatic Fields

The enhancement achieved from exposing a flow to an electrical field has been studied by a large number of researchers. They have demonstrated the enhancement for conventional sized heat exchangers as well as minichannel flows. An excellent paper by Allen and Karayiannis (1995) presents a review of the literature on electrohydrodynamic enhancement. The governing equations, working mechanisms, and existing correlations are presented with some experimental work. It is concluded that the corona wind and electrophoresis contribute the most to single-phase heat transfer enhancement. This technique could also be applied to microchannel flows. In a conventional or a minichannel application, a small insert electrode is present in the flow field. A potential is applied between the insert probe and the channel surface. The electric field that results will provide a moving corona effect and enhance the heat transfer. The possibility of incorporating the electrodes in the walls of a microchannel is quite attractive. The doped region, which forms the electrode, could easily be formed directly in the wall. The electrical connection can be achieved through the substrate of a cover wafer.

3. Flow Pulsation

The variation of the mass flow rate through the channel can also provide heat transfer enhancement. Several researchers have demonstrated the mixing enhancement provided by a pulsating flow. Hessami et al. (2003) studied the effect of flow pulsation on a two-phase flow in a 25 mm pipe. They determined that the enhancement could be as much as 15% depending upon the frequency. This technique could be applied in a microchannel. The requirement of

ISSN (Online) 2456-1290
International Journal of Engineering Research in Mechanical and Civil Engineering (IJERMCE)
Special Issue
National Conference on Advances in Civil and Mechanical Engineering (NCACME 17)

delivering constant mass flow rates to a cooling device could be eliminated.

4. Variable Roughness Structures

Another possibility exists for a variable roughness structure in a microchannel flow. With a variable roughness structure, the heat transfer enhancement could become variable as well. Piezoelectric actuators could be used to control the local surface roughness along the wall. Therefore, the heat transfer enhancement could be customized.

III. EXPERIMENTAL SET-UP OF HERRINGBONE-INSPIRED MICRO STRUCTURES

1. Microfluidic device fabrication and dimensions:-

Microfluidic test devices (Fig. 2) consisting of dry etched microchannels with or without flow promoting structures were fabricated by a series of micro-electro-mechanical systems (MEMS) and integrated circuit (IC) standard fabrication processes in a class 100/1000 clean room. The channels were enclosed with a glass cover by wafer-level anodic bonding. For chemical inertness and electrical insulation 300 nm SiO2 was deposited on both sides of the Si wafer prior to bonding. Up to this point the details of the fabrication process are described in earlier work. After wafer bonding, on-chip resistance temperature detectors (RTDs) were patterned on the backside of the Si wafer. For these RTDs Ti/Au (10/150 nm) was deposited by electron-beam evaporation (Evatec BAK501) and structured by a lift-off process. The necessary soft mask (non-photosensitive lift-off resist underneath positive-tone resist) was backside-aligned to the previously etched channels. In a last step before dicing, mm-size holes for fluidic world-to-chip interfacing were fully etched through the Si wafer (Oxford PlasmaPro 100 Estrelas). In all devices the microfluidic channel had a width of 400 lm. In designs S1-100 and S1-200 the depth of the microchannel was 100 and 200 lm, respectively. In the devices with flow promoters (i.e. S2–S4), the flow promoters had a pitch of 350 lm, a nominal wall thickness of the ridges of 50 lm (i.e. the individual grooves extended over 300 lm downstream) and a height of 100 lm (i.e. the herringbone ridges extended halfway into the overall microchannel height of 200 lm). An additional solid/vacant centreline zone in designs S3 and S4 was 100 lm wide. The flow promoters protruded with an angle of 45_ into the main microfluidic channel.

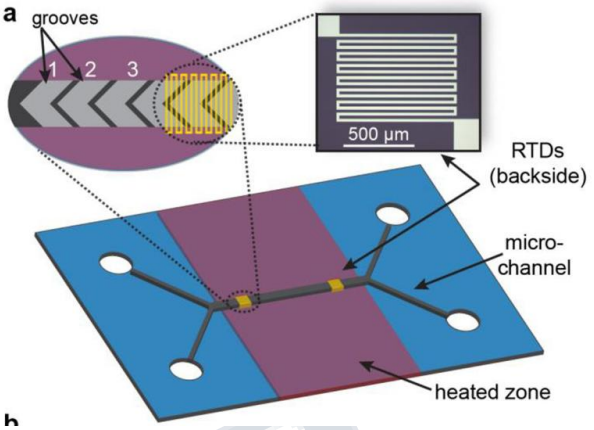

Fig. 2. Microfluidic test chips. (a) Illustration of the microfluidic test chip (front side) including the patterned microchannel and the heated area (thin film heater mounted on the backside), covering the herringbone test-section while leaving space for fluidic world-to-chip interfaces. The resistance thermometers (patterned on the backside) are included as well for illustrative purposes of their position and are also shown as an optical micrograph.

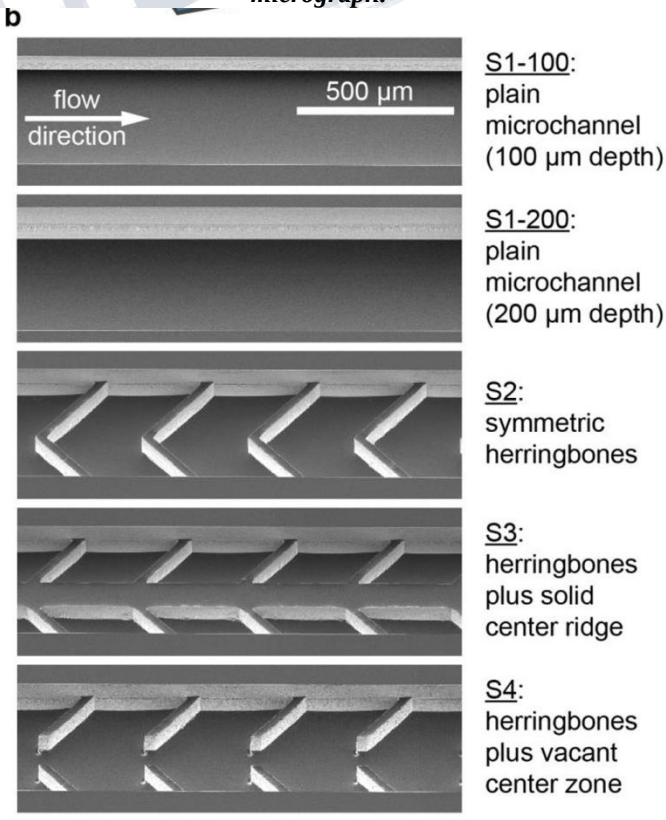

Fig. 2. Microfluidic test chips. (b) Scanning electron microscopy images of the tested microchannels. Design

ISSN (Online) 2456-1290
International Journal of Engineering Research in Mechanical and Civil Engineering (IJERMCE)
Special Issue
National Conference on Advances in Civil and Mechanical Engineering (NCACME 17)

S1-100 is a 100 lm deep microchannel without flow promoters, S1-200 features a 200 lm deep microchannel test section without flow promoters, S2 incorporates symmetric herringbone flow promoters, whereas S3 features an additional solid ridge in the center, which is vacant in design S4. All these flow promoters are of 100 lm height with a total microchannel height of 200 lm. The channel width is 400 lm in all cases.

2. Experimental set-up

Fluidic world-to-chip interfaces were created by a custommade polyphenylene sulfide holder with O-rings as intermediate sealing elements. All tubing was made from chemically inert perfluoroether (Upchurch Scientific). Experiments were performed with 18 MX-cm water and the volume flowrate of the fluid, V was controlled with a syringe pump (Harvard Apparatus PHD Ultra) equipped with two glass syringes of 25 ml each (Hamilton Company). The pressure drop across the flow-promoting zone was measured with a differential pressure sensor (Omega, PD23, 0–2 bar range, ±2 mbar accuracy) on chips with additional pressure taps to the main microfluidic channel. For reporting the pressure drops we converted the differential pressure across the test section, Dp, to the Fanning friction factor:

$$f = \frac{\frac{\Delta p}{\Delta L} \times \frac{{A_c}^3}{P}}{\frac{1}{2}\rho V^2} \quad \text{---------- (1)}$$

During thermal measurements, the test chip was heated with a thin film heater (Minco HR5575) and thermal contact to the chip was ensured using thermal grease. The width of this heater fully covered the herringbone test section, while leaving enough space for the fluidic world-to-chip interfaces. For setting the input power to the heater and data acquisition, electronic terminal blocks were used (Beckhoff Automation AG) which were integrated in a LabVIEW interface. The on-chip RTDs were read out by 4-point probe technique and calibrated in a convection oven against a commercial Pt-100 temperature sensor placed alongside in the holder. In the limited temperature range this calibration data was adequately described by a fit to a polynomial of first degree (see Fig. 3(b), R2 > 99.9) and exhibited a positive slope as expected for metals.

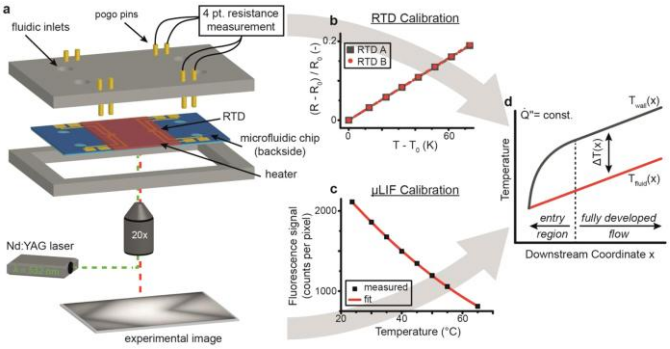

Fig. 3. Experimental set-up and temperature measurements. (a) Illustration of the holder in which the microfluidic test chip is placed during temperature measurements. At the bottom an experimental image is shown as obtained before post-processing. (b) Typical calibration curve of the resistance thermometers. (c) Typical calibration curve of the fluorescence signal in the microchannel. (d) Schematic of the temperature profiles in a microchannel for a constant heat flux.

IV. RESULTS AND DISCUSSION

1. Local temperature distribution

The local fluid temperatures rise linearly as shown in Fig. 4 (open symbols) for all investigated flow rates (same color corresponds to same flow rate) and all channel designs. Here, the dashed line is a linear fit of the measured fluid temperatures. The root mean square (RMS) stays below 1 K for all experiments which indicates a good accuracy of the adopted single-dye lLIF measurement protocol in combination with spatial averaging over the area of a whole groove for each data point. The linear fitting is a further spatial averaging which aids in increasing the accuracy of fluid temperature measurements. This linearity in fluid temperature is in accordance with basic heat transfer theory (c.f. Fig. 3(d)) and strongly verifies the approximation of constant heat flux. The absolute values of the fluid temperatures are of limited physical meaning as we adjusted the heating power to the volume flow rate to yield comparable mean temperatures in the test section (i.e. starting at 6.4W for 2 ml/min we increased the heater power by 5W for every additional 2 ml/min).

However, it becomes already clear that heat transfer is greatly increased by the flow promoters in comparison to the plain channels. First, the slope of the fluid temperature vs. the downstream coordinate $\frac{dT_{fluid}}{dx}$ at the same volume flow is higher for the flow promoting devices S2, S3, and S4 than for the plain channels S1-100 and S1-200. This increase in the steepness of the slope indicates that

ISSN (Online) 2456-1290
International Journal of Engineering Research in Mechanical and Civil Engineering (IJERMCE)
Special Issue
National Conference on Advances in Civil and Mechanical Engineering (NCACME 17)

the heat removal rate Q_{eff} is higher for the flow promoting devices than for the plain channel devices (c.f. Eq. (3), Q_{eff} is directly proportional to dTfluid/dx). This is also shown in Fig. 4(f), in which we plot the heat transfer rate within the test section as function of flow rate for the five considered geometries. Q_{eff} rises significantly with flow rate, which is both a result of increased convective heat transfer and the increase of heater power with flow rate. In all designs containing flow promoting structures (i.e. S2–S4) the coolant takes up much more heat in the test section than in the straight channel designs (S1-100 and S1-200). Also, we notice that Q_{eff} is markedly smaller than the power input to the heater, which is due to the size of the heater covering a larger area than the herringbone test section between groove 5 and 26 and thermal losses from the experimental setup. Apart from the effect on the rate of heat removal, the flow promoters induce a reduction of the temperature difference between the fluid (open symbol) and the RTDs (closed symbol) as seen in Fig. 4(a)–(e). Smaller temperature differences indicate again better heat transfer performance of the flow promoting devices in comparison to the plain channels. The next section quantifies the resulting improvement in heat transfer capability of the channel designs with flow promoters in dimensionless quantities, thus combining both our observations on the heat transfer rates and fluid-to-wall temperature differences.

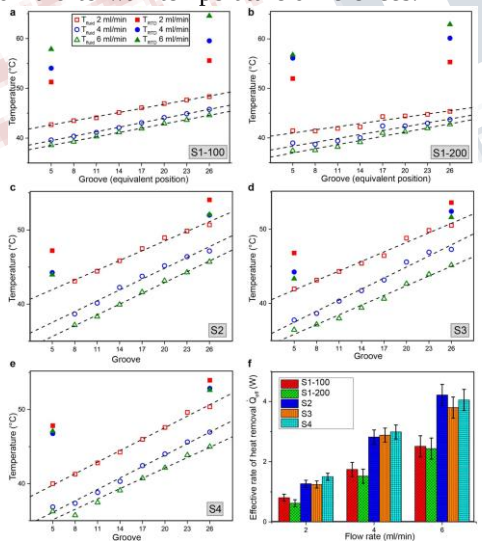

Fig. 4. Fluid and RTD temperatures as a function of downstream coordinate (a–e) and effective rate of heat removal (f). (a) S1-100 (b) S1-200 (c) S2 (d) S3 (e) S4. Dashed lines give a linear fit of the fluid temperature measurements, RTD temperature measurements at grooves 5 and 26 are indicated with a filled symbol. The heater power was adjusted to the flow rates to ensure comparable fluid temperatures in the test section. The legend in (a) is the same for all other temperature measurements shown. (f) Effective rate of heat removal.

2. Mean heat transfer coefficient

Fig. 5(a) compares the average Nusselt number obtained from our measurements of design S1-100 as a function of the nondimensional length scale

$$X^* = \frac{\frac{x}{D_h}}{Re \times Pr} \qquad \text{---------- (2)}$$

to the solutions of Wibuls was compiled by Shah and London , both for a rectangular channel of aspect ratio a = w/h = 0.25 (which resembles the geometry of our test device S1-100 with w/h = 400 lm/100 lm) and a = 0.5. We assume the flow to be hydro-dynamically fully developed as the length upstream of the test section is longer than the expected entrance length (also see discussion on pressure drop below) and thermally developing. Unlike our experiments, in the referred work all four sides of the channel were heated, whereas in the present experiment the top wall was assumed to be adiabatic. For the case of three heated walls at the same aspect ratio, the Nusselt number for both hydro-dynamically and thermally fully developed laminar flow is lower than for the case of no adiabatic wall as shown in Fig. 5(a). The trend in Fig. 5(a) shows that this value is expected to be reached for much longer channels in which the thermally fully developed condition is met (not relevant in this study). For symmetry reasons, we therefore compare our experimental data (three-side-heated, a = 0.25) to the numerical data (four-side-heated) of aspect ratio a = 0.5 and observe good agreement. In both cases the temperature gradient vanishes at the same height (mid-height of the channel with 4 heated walls). This makes the thermal boundary conditions of our problem with 3 heated sides (a = 0.25) and of half of that problem with 4 heated sides (a = 0.5) from the literature identical (see Fig. 5(b)), which is the most important consideration for this comparison regarding heat transfer. These considerations substantiate the consistency of our experimental data with conventional heat transfer theory. We believe that the measurement of the local fluid temperature by optical means as we perform in this work and the subsequent spatial fitting of the obtained temperature readings along the downstream coordinate results in more accurate estimates of the Nusselt number than probing the fluid temperature with thermocouples. These probes are often only sparsely placed at distinct positions, hence the assumed boundary conditions cannot be verified by the downstream temperature distribution. Moreover, such probes inevitably change the local flow pattern due to the usually large size of the probe in comparison to the characteristic size of the microchannel.

ISSN (Online) 2456-1290
International Journal of Engineering Research in Mechanical and Civil Engineering (IJERMCE)
Special Issue
National Conference on Advances in Civil and Mechanical Engineering (NCACME 17)

After validating our methodology with the data on S1-100, we now study the effect of flow promotion on the Nusselt number (see Fig. 5(c)). Here, the base case is S1-200 which features a microchannel depth of 200 lm without any ridges and is of same hydraulic diameter as the devices with flow promoters (i.e. S2– S4). The height increases stepwise in device S1-200 from 100 lm to 200 lm at a location equivalent to the start of the grooved section in designs S2–S4. This step triggers a hydraulic instability, as it is the case with flow promoters, and the flow is at the same time hydro-dynamically and thermally developing. The observed mean Nusselt numbers for 2, 4 and 6 ml/min (Re = 190–510) are 4.4, 6.6 and 9.2 in S1-200, respectively. In direct comparison we observe much higher Nusselt numbers for the same flow rates in all designs containing flow promoters. Specifically, the corresponding mean Nusselt numbers in design S2 are 18.4, 32.2 and 36.6. A direct comparison of the Nusselt numbers in S2 to S1-200 shows an impressive improvement by a factor of about 4 or higher. This fourfold improvement seems to be in general accordance with the work by Yang et al. on herringbone structures and is remarkable as it proves that herringbones are a viable alternative to well-studied arrays of pin-fins, showing a similar enhancement of Nusselt number upon the onset of vortex shedding. The results on design S3 show Nusselt numbers slightly lower than for device S2. This is expected as this device S3 incorporates a continuous central ridge. In previous work we showed that the flow above this central ridge remains largely stratified while convective mixing occurs away from it. Therefore, it only seems logical that the performance in terms of Nusselt number of design S3 remains lower than in design S2 in which the vortices span along the whole width of the channel. Device S4 performs even lower than S3 in terms of Nusselt number. Re-examining Fig. 4(e) we observe that the temperature difference between fluid and wall is distinctly larger at groove 5 than at groove 26, i.e. design S4 shows much larger entrance effects than the other two designs featuring herringbones (i.e. S2 and S3). It appears therefore that the vacant center zone of design S4 hinders the mixing effect of the flow promoters to break up the thermal boundary layer in the entrance of the grooved section. Such entrance effects are much less visible for designs S2 and S3 (c.f. Fig. 4(c) and (d)), which in combination with the higher Nusselt numbers renders these two designs attractive for cooling of local heat spots.

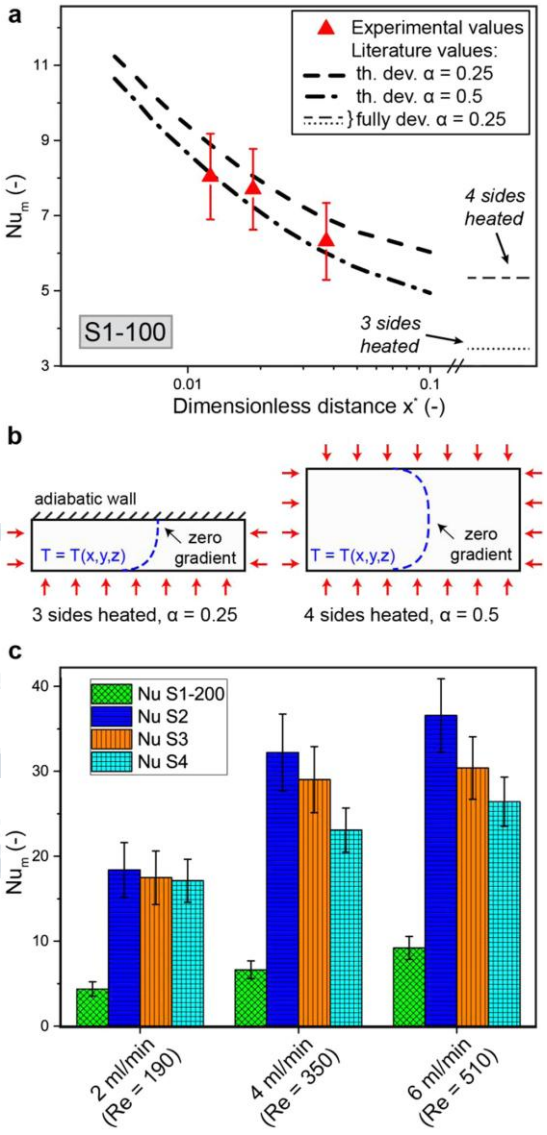

Fig. 5. Average Nusselt numbers. (a) Average Nusselt number for S1-100 as a function of the dimensionless downstream coordinate x⁄ (c.f. Eq. (8)). The bold dashed and dashed-dotted lines show for thermally developing flow and aspect ratios a of 0.25 and 0.5, respectively, but for four heated walls. For thermally fully developed flow (i.e. infinite x⁄) the data for a = 0.25 and both 4 and 3 heated walls is plotted using thin lines. (b) Schematic illustration of the temperature profiles for the cases of three (a = 0.25) and four heated walls (a = 0.5). (c) Average Nusselt number comparing designs S1-200, S2, S3, and S4 at the three different flow rates.

ISSN (Online) 2456-1290
International Journal of Engineering Research in Mechanical and Civil Engineering (IJERMCE)
Special Issue
National Conference on Advances in Civil and Mechanical Engineering (NCACME 17)

3. Pressure drop and figure of merit.

Fig. 6 presents our measurements of the pressure drop in terms of the non-dimensional Fanning friction factor (c.f. Eq. (1)). Again, our measurements for S1-100 are well correlated to laminar theory of hydro-dynamically fully developed flow in rectangular crosssections: The solid line shows the analytical solution in a rectangular microchannel of dimensions 400 _ 100 lm2 and fits our experimental data well. In the given range of Re numbers we observe strictly fully-developed laminar flow for device S1-100 as concluded from the agreement of our measurements with laminar theory. Test chip S1-200 shows slightly higher friction factors than design S1-100, which seems to be counterintuitive because laminar theory would predict a lower friction factor. However, the flow in design S1-200 experiences a step change (from 100 to 200 microns in height at the entrance, as mentioned earlier) and accounting for both these effects, we use the following definition as a figure of merit

$$FOM = \frac{\mathrm{N_{um}}}{\frac{N_{um,S1-200}}{\frac{f}{f_{S1-200}}}} \quad \text{---------- (3)}$$

as suggested by Webb and Eckert and since then used frequently both in original research articles and review articles. This definition of a FoM relates the augmentation of thermal performance of the ribbed microchannels against the plain microchannel S1-200 of same hydraulic diameter at equal surface area and pumping power. For all considered flow promoting designs S2, S3, and S4 and all flow rates, the FoM is well above unity indicating a net performance enhancement in heat transfer despite the increased flow resistance. The highest value is reached by design S4 at 2 ml/min with 250%, which is due to the relatively low friction factor in this design. For the device S2 reaching the highest Nusselt numbers in this study, the FoM is maximal at 4 ml/min at a value of 220%. For higher flow rates of 6 ml/min the FoM decreases for all designs due to the less favourable development of Nusselt number and friction factor as also found on pin-fin arrays. Yet, in direct comparison to electronic cooling concepts by pin-fin arrays, our highest measured FoM is substantially increased due to the reached augmentation in Nusselt number. This is also in agreement with the data compiled by Ligrani et al. for macroscale internal heat transfer, which indicates that the obtainable thermal performance as measured by Eq. (3) is generally much higher for rib turbulators than for pin fins.

V. CONCLUSION OF EXPERIMENTAL SET UP

This work reports on the heat transfer enhancement caused by herringbone flow promoters in ribbed microfluidic channels. We obtain a four-fold increase of Nusselt number in comparison to a smooth channel. Accounting also for the additional pressure losses by using the thermal performance ratio

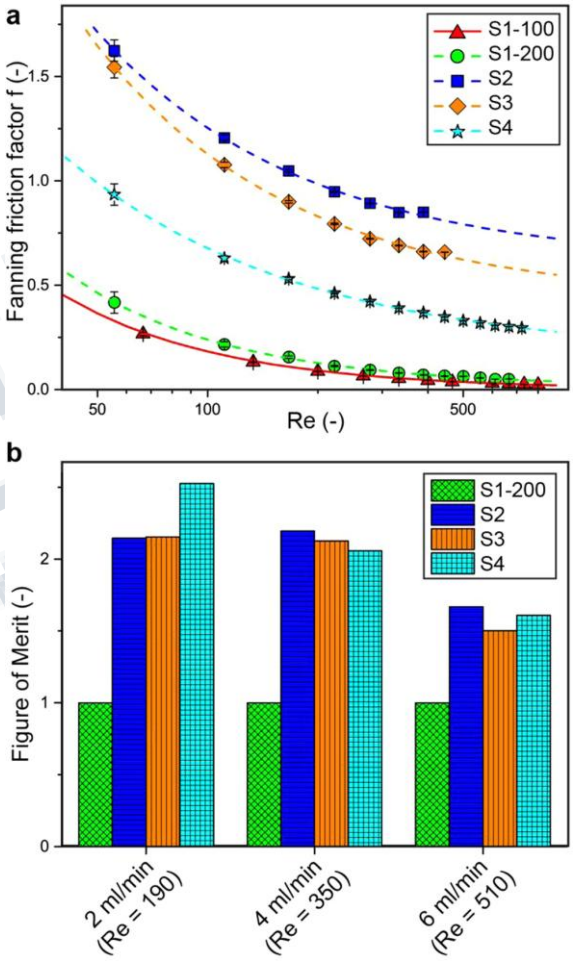

Fig. 6. Fanning friction factor and figure of merit. (a) Fanning friction factor as function of Reynolds number. The solid line is the analytical solution for the dimensions of microchannel S1-100 . The dashed lines are fitted to the experimental data. (b) Figure of merit for the three tested flow rates for different microchannels configurations.

$$FOM = \frac{\frac{N_u}{N_{uo}}}{\{\frac{f}{f_o}\}^{\frac{1}{3}}}$$

ISSN (Online) 2456-1290
International Journal of Engineering Research in Mechanical and Civil Engineering (IJERMCE)
Special Issue
National Conference on Advances in Civil and Mechanical Engineering (NCACME 17)

which compares the Nusselt number in a herringbone microchannel to a smooth microchannel at same pumping power and surface area, we gain a maximum overall improvement of 220% at 4 ml/ min (Re = 350) for the design S2 with the highest Nusselt number. At this operating point the Nusselt number itself already rises to 32.2 as compared to 6.6 for the device without flow promoters. At a Reynolds number of 510 the Nusselt number in design S2 increases even further to 36.6. We find that design S2 with symmetric herringbones across the entire microchannel width results in the highest heat transfer enhancement in comparison to the other devices, due to the most rigorous flow mixing. Although in the same device (design S2) the Fanning friction factor is highest, the heat transfer augmentation greatly outperforms the adverse pressure effects. Only at low flow rates of 2 ml/min the designs with an additional vacant zone at the centerline (design S4) show a higher heat transfer benefit compared to corresponding pressure losses, i.e. the FOM is higher due to the lower pressure drop.

VI. CONCLUSION

The following conclusions can be drawn from the present work. Some of the more successful enhancement techniques currently used for heat transfer augmentation have been reviewed. The applicability of single-phase enhancement techniques is evaluated for microchannel and minichannel flows. Several passive techniques have been identified as possibilities for microchannel enhancement. The passive techniques do not rely on external power or activation. Therefore, these techniques do not have any additional power costs.

Several active techniques have been identified as possibilities for microchannel enhancement. Unfortunately, these techniques do require external power. There is a power cost that needs to be considered. This fact makes a microsystem designer carefully consider their implementation. Pressure drop penalties and heat transfer performance of the enhancement techniques discussed in the present work need to be verified experimentally and/or numerically. There is a great deal of research needed to bring these proposed techniques into fruition. In some cases, the technology might not be available. However, the present work is expected to serve as a road map for microchannel and minichannel heat transfer enhancement.

It concludes that herringbone microstructures are an attractive class of flow promoters for enhanced heat transfer in microchannels. We expect beneficial applications of such herringbone flow promoters in electronics cooling, in which high local heat loads need to be dissipated by a coolant. Single-phase cooling concepts of this kind have inherent advantages regarding the ease and reliability of operation and maintenance. In addition, advanced new concepts of integrated cooling and simultaneous power delivery require operation in the single-phase regime. In these cases, the combined heat and mass transfer enhancement is expected to yield both better thermal performance as well as higher diffusion-limited currents. In fact, the effects of flow promotion occur on both the structured and unstructured sides of fluidic channels as shown in our present and past work. Thus, this contribution has important implications for heat transfer as well as microfluidic reactor design, and represents an important step forward on the way toward green cloud and high performance computing.

REFERENCES

[1] “Single-Phase Heat Transfer Enhancement Techniques In Microchannel And Minichannel Flows”; Mark E. Steinke[1] And Satish G. Kandlikar[2] (1thermal Analysis And Microfluidics Laboratory, Mechanical Engineering Department, Rochester Institute Of Technology), Microchannels And Minichannels – 2004 June 17-19, 2004, Rochester, New York, Usa.

[2] “Theoretical and Experimental Investigation of Heat Transfer Characteristics through a Rectangular Microchannel Heat Sink”; Dr. B. S. Gawali 1, V. B. Swami, (Professor Dr., Department of Mechanical Engineering, Walchand College of Engineering, Sangli), Vol. 3, Issue 8, August 2014.

[3] “Analysis of three-dimensional heat transfer in micro-channel heat sinks”,(Weilin Qu, Issam Mudawar, (Boiling and Two-phase Flow Laboratory, School of Mechanical Engineering, Purdue University, West Lafayette, IN 47907, USA), International Journal of Heat and Mass Transfer 45 (2002).

[4] “Single-Phase Liquid Heat Transfer In Plain And Enhanced Microchannels”; Mark E. Steinke[1] And Satish G. Kandlikar[2] (1Thermal Analysis And Microfluidics Laboratory, 2Mechanical Engineering Department, Rochester Institute Of Technology), Fourth International Conference On Nanochannels, Microchannels And Minichannels June 19-21, 2006, Limerick, Ireland.

[5] “Significant heat transfer enhancement in microchannels with herringbone-inspired microstructures”; Julian Marschewski a,b, Raphael Brechbühler a, Stefan Jung a, Patrick Ruch b, Bruno Michel b, Dimos Poulikakos a, (a Laboratory of Thermodynamics in Emerging Technologies, Department of Mechanical and Process Engineering, ETH

Zürich, 8092 Zürich, Switzerland, b IBM Research Zurich, Säumerstrasse 4, 8803 Rüschlikon, Switzerland), International Journal of Heat and Mass Transfer 95 (2016) 755–764.

[6] "Study of Fluid Flow and Heat Transfer Through Mini-Channel Heat Sink"; Hemant Kumar1 and S.S.Sehgal2, (1University College of Engineering, Punjabi University, Patiala, Punjab -147 002, India, 2Department of Mechanical Engineering, Chandigarh University, Mohali, Punja),Asian Journal of Engineering and Applied Technology Vol. 2 No. 2, 2013, pp. 25-28.

[7] "Microchannel Heat Exchangers – Present And Perspectives";Traian Popescu, Mircea Marinescu, Horaţiu Pop, Gheorghe Popescu, Michel Feidt, (Department Of Applied Thermodynamics, Engines, Thermal And RefrigeratingEquipment, Faculty Of Mechanical Engineering And Mechatronics, University Politehnica Of Bucharest, Romania), U.P.B. Sci. Bull., Series D, Vol. 74, Iss. 3, 2012.

[8] "A review on enhancement of heat transfer in microchannel heat exchanger"; Lokesh Chandra Joshi, Dr. Satyendra Singh, Shailesh Ranjan Kumar ,(Department of Mechanical Engineering, BTKIT Dwarahat, Almora, Uttarakhand, India), IJISET - International Journal of Innovative Science, Engineering & Technology, Vol. 1 Issue 9, November 2014.

[9] "Investigation of heat transfer in rectangular microchannels"; Poh-Seng Lee, Suresh V. Garimella, Dong Liu,(Cooling Technologies Research Center, School of Mechanical Engineering, Purdue University, 585 Purdue Mall, West Lafayette, Indiana), International Journal of Heat and Mass Transfer 48 (2005) 1688–1704.

[10] "Flow Boiling Heat Transfer in Microchannels"; Dong Liu1, Suresh V. Garimella,(Cooling Technologies Research Center, School of Mechanical Engineering, Purdue University, West Lafayette, IN 47907-2088), Journal of Heat Transfer ASME OCTOBER 2007, Vol. 129.

[11] "High Flux Heat Removal with Microchannels—A Roadmap of Challenges and Opportunities"; SATISH G. KANDLIKAR (Thermal Analysis and Microfluidics Laboratory, Rochester Institute of Technology, Rochester, NY, USA,) Heat Transfer Engineering, 26(8):5–14, 2005.